A Novel Robot Gripper with Scott Linkage for Scooping and Self-Adaptive Grasp in Environmental Constraints

Shijie Qu[1] and Wenzeng Zhang[2*]

[1] Lab of Robotics, X-Institute; School of Big Data and Internet, Shenzhen Technology Univ., Shenzhen, China. (qushijie644@gmail.com)

[2] Lab of Robotics, X-Institute, Shenzhen; Dept. of Mechanical Engineering, Tsinghua Univ., Beijing, China (email: wenzeng75@163.com) * Corresponding author

Abstract: This paper proposes an adaptive finger mechanism for environmental constraints. The mechanism is based on the coupling of Scott linkages and passive elastic elements and is controlled by a single linear driving device to achieve composite grasping functions such as pinching, bimodal scooping (symmetrical scooping and asymmetrical scooping) and adaptive enveloping. The proposed finger mechanism is more concise compared to previously developed mechanisms, can be installed on existing commercial robotic arms and has lower production costs. This mechanism utilizes the linear motion characteristics and geometric constraints of the Scott linkage, combined with spring limit, to achieve vertical flexibility in the face of environmental constraints and can adaptively grasp objects of different shapes, materials and positions. Especially in the symmetrical scooping configuration, it can effectively grasp large thin objects such as cards; Under asymmetric configuration, the stability of sheet grasping is improved by tilting the gripper. This study provides new ideas for the design of low-cost, high-precision environment adaptive grippers and expands the potential application of the underactuated robotic gripper in complex environments.

Keywords: Robot gripper; Self-adaptive grasping; Pinching; Scooping; Scott linkage

1. INTRODUCTION

As the core component of robots to perform operations, the adaptive grasping ability of robotic hands directly affects the reliability of tasks in complex scenes. In traditional solutions, industrial grippers rely on structured environments and high - precision control [1], dexterous hands have high flexibility but are expensive [2] and special grippers are limited to specific scenarios. How to achieve a balance between complexity, cost control and environmental adaptability has become the key to breaking through environmental constraints.

The underactuated mechanism is designed through the coupling of elastic elements and transmission, achieving multi-DOF compliance with a small number of actuators, providing a new approach for adaptive grasping. Birglen [3] systematically elucidated the mechanical modeling method of underactuated mechanisms, laying a theoretical foundation for subsequent design. The compatible mechanism proposed by the Dollar [4] achieves passive adaptation through distributed compliance characteristics but has limitations in vertical compliance. The MARS Hand was developed by Gosselin with dual modes of parallel pinching and adaptive grasping [5]; A new underactuated finger with multi-DOF adaptive grasping capability developed by Feng [6]; The linear parallel pinching and coupled adaptive robotic hand LPCSA [7] that can grip objects in multiple grasping modes.

Although these studies have made significant progress in the development of underactuated devices and adaptive functions, which have not effectively solved the problem of rigid fingers grasping objects under environmental constraints. In practical applications, rigid hands require high control accuracy due to wear and tear caused by collisions with the environment. In recent years, with the advancement of sensor technology, control algorithms, materials science and mechanism design, adaptive grasping technology has made significant progress.

The development of soft robotic hands has also become a much-focused research direction. The pneumatic actuator developed by the Harvard Univ. [8] can achieve biomimetic bending motion; The RBO soft hand [9] by MIT achieves passive compliance through silicone material; The origami-structure pneumatic actuator developed by the Shepherd [10] further enhances the efficiency of soft driving. However, although soft robots have passive compliance, they face problems such as insufficient driving force, slow dynamic response and complex nonlinear control [11]. Although the rigid-flexible fusion design can partially compensate for the shortcomings (such as the biomimetic octopus tentacle [12] by Beihang Univ.), it still relies on external driving or complex sensing systems [13], deviating from the original intention of passive under-actuation design.

Fig. 1. The Gamma gripper.

Faced with the problem of insufficient mechanical compliance of rigid actuators under environmental

constraints, Yoon adopted a robotic hand coupled with Hart linkage and parallelogram mechanism [14]. Through ingenious mechanism design, it can achieve stable scooping in complex environments and interact with the environment through vertical compliance and posture switching. It spontaneously generates adaptive scooping movements when it contacts the physical environment and has good physical intelligence.

This paper proposes an underactuated gripper design based on the Scott linkage and it is named the "Gamma" gripper because the mechanism resembles upside down of the Greek letter γ (gamma).

The Gamma gripper retains the advantages of the Omega gripper [14], such as object adaptation, vertical environmental compliance, easy installation and dual-mode scooping. Its prominent features include:

1) Simplification of the mechanism: By utilizing the linear motion characteristics of the Scott linkage, a simplified four-link mechanism replaces traditional multi-link mechanisms (such as Hart linkage), directly producing precise vertical trajectories. The overall structure is concise, eliminating complex parameter constraints.

2) Cost optimization: With a simple mechanism that can be directly produced through 3D printing. With fewer connecting rods, it is easy to install [15].

3) Ability enhancement: In addition to the vertical flexibility of the fingertips, the Gamma gripper also has strong adaptive enveloping ability, especially for irregular objects.

In Part II of this article, the relevant research work on underactuated hands is introduced. In Part III, the mechanical structure of the Gamma gripper is presented. In Part IV, the key factors determining whether the Gamma gripper can achieve the scooping function are analyzed. In Part V, grasping experiments will be conducted. Finally, in Part VI, a summary will be provided.

2. RELATED WORK

The current research on adaptive grasping of robotic hands can be divided into three technical routes: rigid underactuated mechanisms, soft and rigid flexible hybrid mechanisms and environment-driven mechanisms.

Rigid underactuated mechanisms often achieve passive adaptation by combining kinematic constraints with elastic elements. The innovation trend is mainly reflected in the combination of flat clamping, coupling and adaptive gripping methods to achieve functional diversity, such as the mechanical structural changes shown in the Feng mechanism topology periodic table [6]. Some researchers have also modified the original gripping methods, such as Luo, who achieved flat clamping adaptation of fingertips through structural design [16], solving the problem of fingertip curvature at the end and making gripping positioning more stable and accurate. However, rigid structures are prone to collisions with the surface of objects during use, which can lead to accumulated errors. Complex linkage mechanisms often have high costs and are difficult to maintain in a timely manner, resulting in a decrease in finger grasping ability.

Soft and rigid flexible hybrid mechanisms break through the constraints of rigidity through material innovation and the shaping of soft structures, demonstrating unique value in interacting with the environment and human–machine interaction. Early representative works, such as the pneumatic actuator proposed by Deimel and Brock [17], first applied the PneuNet folded structure to robotic hand design. Subsequently, the team further developed an underactuated compliant hand [9], which achieved multi-finger collaborative grasping through a parallel topology design of air chambers. The Pisa/IIT Soft Hand developed by the Catalano team [18] can also achieve good grasping effects through the synergistic effect of tendon–pulley coupling and flexible joints. However, soft robotic hands still face issues such as complex driving devices, slow response speeds and material creep leading to decreased motion accuracy [19].

Environment-driven research takes a different approach by transforming external constraints into grasping potential energy. The vertical flexibility design of the OMEGA gripper [14] breaks through the bottleneck of environmental interaction—when the fingertip touches the tabletop, the geometric constraint of the Hart linkage spontaneously triggers the scooping action, successfully grasping credit cards with a thickness of less than 1 mm.

This article aims to reconstruct the kinematics based on the OMEGA gripper: the Scott linkage replaces the Hart linkage, maintaining good environmental adaptability while reducing the number of linkages and mechanism costs, in order to face grasping tasks in different situations.

3. THE GAMMA GRIPPER

3.1 Scott linkage Mechanism

The Scott mechanism, also known as the connecting rod chute mechanism, is characterized by its ability to generate precise linear motion.

Its operating principle is shown in Fig. 2a. The key feature of this mechanism is that $l_b = 2l_a$. The mid - point B of the CD connecting rod lies on the circumference with A as the center and r (where r is a specific radius value) as the radius and the straight line AC is always the chord of the circle with B as the center and r (the radius here may have a specific relationship with the above - mentioned r, which needs to be determined according to the specific context) as the radius. It is precisely based on such geometric relationships that precise linear motion is achieved.

3.2 Design of the Gamma Mechanism

Fig. 2b shows the relationship between Δh and $\Delta\theta$ when the Scott linkage is in vertical motion.

We define the linkage parameters as follows: l_{AB}, l_{CB} and l_{AD} represent the length of the first finger segment, the second finger segment and the distance between the

origin and the slide rail respectively. l_{CD} is the drive linkage, which enables the tip point C to move precisely along a straight line.

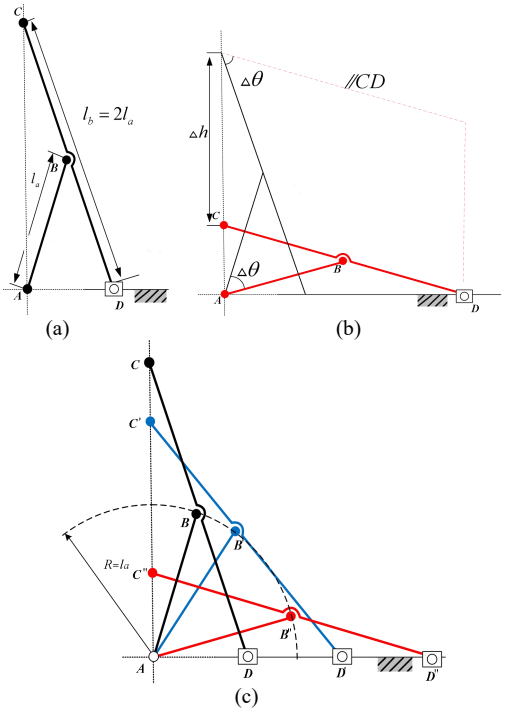

Fig. 2. The principle of the Scott Mechanism.

The relationships among the parameters of these linkages can be obtained through formulas, so as to better set the initial state of the fingers and enable the fingers to better respond to external forces.

The mechanical characteristics of the Scott mechanism itself are:

$$l_{CD} = 2l_{AB} \tag{1}$$

In the initial state, l_{AD} satisfies the following relationship:

$$l_{AD} = 2l_{AB}\cos\angle BAD \tag{2}$$

The distance l_{AC} from the distal joint axis to the finger base satisfies:

$$l_{AC} = 2l_{AB}\sin\angle BAD \tag{3}$$

Set the length of the first finger segment as previously determined l_{AB} = 50 mm, ∠BAD = 70°, The corresponding values of l_{AD} = 34.2 mm and l_{AC} = 93.97 mm, along with l_{AB}, l_{AD}, l_{AC}, l_{CD} and angle ∠BAD, are stored in Table 1.

Table 1. Dimension Parameters of the Gamma finger

Predetermined parameters			Designed parameters	
l_{AB}	l_{CD}	∠BAD	l_{AC}	l_{AD}
50mm	10mm	70°	93.97mm	34.2mm

In addition, as shown in Fig. 3, a spring k_1 is installed at joint B to enable the finger to extend after bending, achieving its compliance. A stopper Q_1 is set at joint A, with Q_1=20°, to ensure the stability of the finger's initial state.

3.3 The implementation of the scooping.

As shown in Fig. 3, the parallelogram mechanism and the Scott mechanism share joints A, B and C. This arrangement makes the overall structure of the finger more compact. The stability of the parallelogram when gripping flat objects allows a pair of Gamma mechanisms to grasp objects more stably.

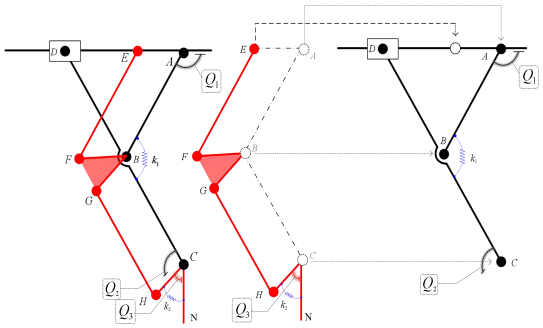

Fig. 3. Gamma finger with Scott and parallelogram linkages.

The fingertip of this manipulator can achieve two scooping postures in coordination with the robotic arm. Scooping can guide objects that cannot be directly grasped by flat clamping into the range where the gripper can grasp them and then perform pinching or enveloping operations.

A stopper Q_2 is set on link CD and a stopper Q_3 is set on link CH, with the angle designed as Q_3 = 52.5°(∠FBG=40°). It works with spring k_2 to provide vertical support for fingertip CN. Q_2 is the key to triggering the scooping posture and its function and the conversion process of the scooping posture are shown in Fig. 4.

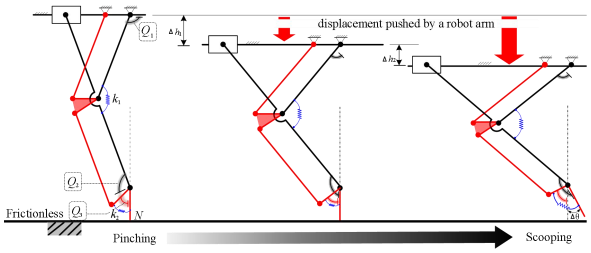

Fig. 4. The fingertip posture transition from parallel pinching to scooping is achieved by the push of the stopper.

As shown in Fig. 4, when the gripper is pushed downward and the height difference has not reached Δh_1, Q_3 and k_2 can provide good support. When the height displacement reaches Δh_1, Q_2 comes into contact with the fingertip. Further downward pressure can cause Q_2 to push the fingertip to one side, forming an angle of attack, while overcoming the pressure of spring k_2. We can refer to $0 \le h \le \Delta h_1$ as the flat clamping range.

When the height displacement reaches and joint D reaches the end of the guide rail, the scooping posture is completed. We can refer to $\Delta h_1 \le h \le \Delta h_2$ as the scooping range. The angle of Q_2 is set to 150°. The size of the angle of attack is related to the angle setting of Q_2 and the length l from the origin to the end of the track, satisfying:

$$\cos\theta = l/(2l_{OC}) \tag{4}$$

$$\theta = \arccos\theta \tag{5}$$

$$\Delta\theta = Q_2 - 90^\circ - \theta \tag{6}$$

Let the length l be 86.6 mm, at which point, when in the scooping posture, θ is exactly 30°.In this case, $\Delta\theta$ = 30 ° . All dimensions of the parallelogram and the stoppers are listed in Table 2.

Table 2. The Parallelogram Mechanism and the Stopper.

Q_1	Q_2	Q_3	θ,Δθ	∠FBG	AE,BF,CH,BG	CN
20°	150°	52.5°	30°	34.2mm	20mm	30mm

4. MECHANISM ANALYSIS

4.1 Core Mechanism of the Scooping Function

The device's core function is stable scooping, with its key mechanism being coordinated motion between stopper Q_2 and the distal fingertip during scooping. To ensure reliability, when the robotic arm presses into the target range, Q_2 must continuously push the fingertip to form a stable angle of attack with no relative displacement. This constraint, a static equilibrium issue, is achieved via rational configuration of the fingertip's constrained force system, particularly spring elastic coefficient k_2.

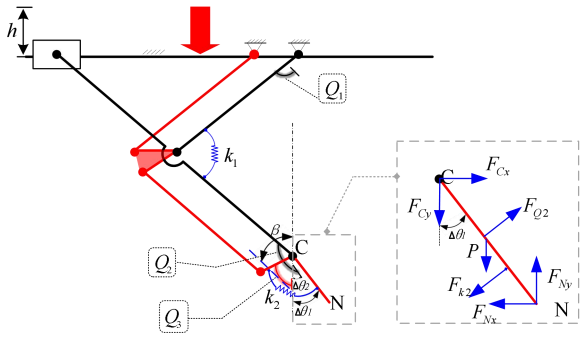

Fig. 5. Forces acting on the fingertip CN.

4.2 Theoretical Analysis of Fingertip Forces

In the theoretical analysis, the forces acting on the distal phalanx can be simplified as a planar force system model (Fig. 5). The figure annotates the primary forces and constraints: the axial thrust from Q_2 (F_{Q2}), the elastic restoring force of spring k_2(F_{k2}), the reaction force from the tabletop (N) and the support force at revolute joint C (F_C). When the robotic arm presses downward, the thrust from Q_2 is transmitted through the linkage to the fingertip, forcing the phalanx to rotate about axis C and form the desired angle of attack for contact with the target object. During this process, spring k_2 must provide resistance matching F_{Q2} to maintain static equilibrium of the phalanx. If k_2 is too large, the excessive spring stiffness will hinder the downward motion of the robotic arm, causing mechanism jamming or damage; if k_2 is too small, the thrust from Q_2 cannot overcome the spring deformation, resulting in relative slippage between the fingertip and Q_2, thereby destabilizing the angle of attack. Based on the planar force equilibrium conditions:

$$\begin{cases} \sum F_x = F_{Q2} - F_{k2}\cos\beta - F_{Cx} = 0 \\ \sum F_y = N - F_{k2}\sin\beta - F_{Cy} = 0 \\ \sum M_C = F_{Q2}\cdot d_1 - F_{k2}\cdot d_2 = 0 \end{cases} \tag{7}$$

The installation angle β of the spring affects the direction and magnitude of the spring force in the overall mechanical structure. The moment arm d_1 of Q_2 thrust, which is the perpendicular distance from the Q_2 axis to the rotation center C, and the moment arm d_2 of spring k_2, which is the perpendicular distance from the spring action line to C, are crucial geometric parameters that determine the torque generated by the forces in the system. However, due to space limitations, the distances d_1 and d_2 are not marked in the figure.

The elongation of the spring caused by the motion of the linkage is calculated as follows:

$$\Delta l_{k2}(\theta) = l_{CD}[\cos(\angle BAD - \theta) - \cos(\angle BAD)] \tag{8}$$

where $\theta \in [20^\circ, 90^\circ]$ denotes the joint rotation angle. This geometrically nonlinear relationship ensures precise force-displacement coupling during scooping. From moment equilibrium about joint C:

$$F_{Q2}(\theta) = k_2\cdot\Delta l_{k2}(\theta)\cdot d_2/d_1 \tag{9}$$

This reveals the linear proportionality between driving thrust and spring stiffness, constrained by $\Delta l_{k2} > 0$ for effective engagement. The design criterion for the spring stiffness is given by the following equation:

$$k2 = F_{Q2}\cdot d_1/\Delta l_{k2} d_2 \tag{10}$$

4.3 Grasping Force Modeling

$$Fg(\theta) = \underbrace{\frac{k_2\cdot\Delta l_{k2}(\theta)\cdot d_2}{d_1}}_{F_{Q2}\ contribution} + \underbrace{\mu\cdot k_2\cdot\Delta l_{k2}(\theta)}_{Spring\ friction\ effect} \tag{11}$$

The pinching force can be described as a composite force composed of the Q_2 thrust and frictional effects. Its expression is where μ represents the friction coefficient between the silicone fingertip and the object. This pinching force is an important part of the overall grasping force mechanism.

The shovel force, on the other hand, can be described as a force calculated based on the normal reaction force and the attack angle. The normal reaction force during scooping is

$$N(\theta) = k_2\cdot\Delta l_{k2}(\theta)\cdot\sin\beta + F_{Cy} \tag{12}$$

The shovel force is then obtained as:

$$F_s(\theta,\phi) = N(\theta)\cdot\tan\phi \tag{13}$$

where ϕ denotes the attack angle determined by the Q_2 geometry. It plays a crucial role in the scooping operation of the gripper.

The total grasping force can be described as the coupling result of the pinching force and the shovel force. Its formula is

$$F_t(\theta,\phi) = F_g(\theta) + \alpha\cdot F_s(\theta,\phi) \tag{14}$$

5. GRASPING EXPERIMENTS

To verify the design concept proposed in this paper, we designed a prototype and conducted grasping experiments with it to validate the three grasping methods of the Gamma mechanism. The entire prototype was printed using the Bamboo Lab A1 printer. PLA (elastic modulus: 3.5 GPa, tensile strength: 50 MPa) was prioritized in material selection because it strikes the best balance between cost-effectiveness and functional requirements.

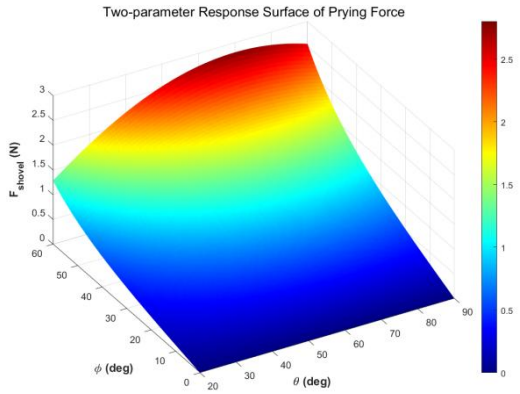

Fig. 6. Response surface of Force (F) versus inclination angle (θ)

5.1Prototype Design

As shown in Fig. 7, a 2-mm-deep groove is designed on the contact surface between the Gamma fingertip and the object and a 2-mm-thick textured silicone plate is bonded inside the groove to optimize the surface interaction. Compared with the bare PLA material, the textured silicone plate can provide greater friction, making the grasping more stable. Meanwhile, its elasticity allows it to better simulate the mechanical characteristics of human fingertips.

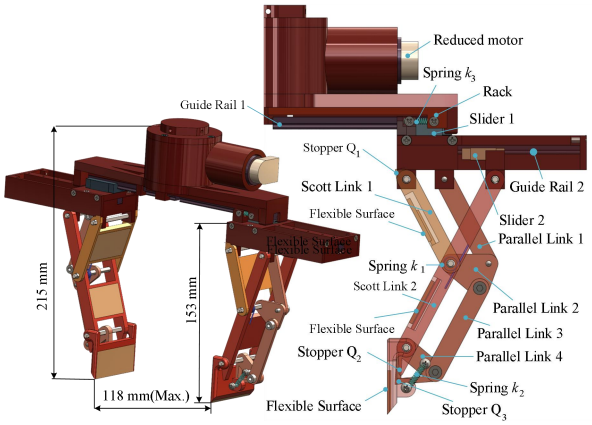

Fig. 7. Overall view of the Gamma gripper.

5.2 Spring Selection

Through experimental verification, we have found that improper spring design can lead to three scenarios. When the elastic force of spring k1 is too large, during the pressing process, the Gamma mechanism is not prone to vertical compliance, which can easily lead to rigid collisions (as shown in Fig. 8a) and it is also difficult to achieve the adaptive functionality of the object (as shown in Fig.11). As depicted in Fig. 8b, when the elastic force of spring k_2 is too small, it is insufficient to provide the fingertip recovery force and thus cannot support the stability of the scooping grasp.

(a) (b)

Fig. 8.Different springs on the Gamma gripper.

5.3 Parallel grasping and symmetrical scooping.

The prototype machine can complete parallel grasping and symmetrical scooping operations on smooth surfaces, as shown in Fig. 9. In the parallel grasping mode, it can successfully grasp objects such as a miniature wrench and a thin card. In the case of symmetrical scooping, it can achieve adaptability for cylindrical objects, successfully adjusting the paper cup to a position suitable for enveloping grasp. At the same time, this gripper can also grasp irregular objects through the first and second phalanges. Fig. 9 also compares the different grasping results in the parallel grasping and scooping states.

(a) The Gamma gripper performs parallel grasping of the object.

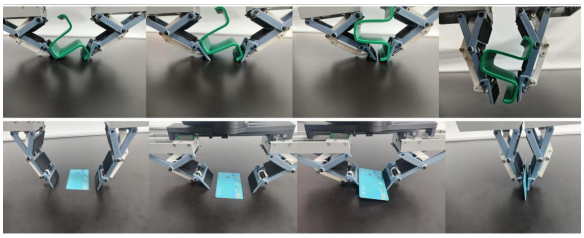

(b) Gamma symmetrical scooping of an object.

Fig. 9. Grasping experiments on the Gamma gripper

5.4 Asymmetric Scooping and Inclined Surface G rasping

As shown in Fig. 10a: Arm tilting fixes one fingertip while sliding the opposing fingertip beneath via attack angle to lift. Fig. 10b: Height difference and friction enable asymmetric grasping on inclines .

(a) Picking up a card through asymmetric scooping.

(b) Picking up an object on an inclined surface.

Fig.10. Asymmetric scooping, as well as picking up an object on an inclined surface.

5.5 Adaptive Envelopments

As shown in Fig. 11, the prototype of the Gamma gripper, by selecting appropriate torsion springs, endows the gripper with a good adaptive capability, enabling it to adapt to irregularly shaped objects and perform stable enveloping.

Fig. 11. Adaptive enveloping of the Gamma gripper.

6. CONCLUSIONS

This paper proposes design of a novel gripper, Gamma gripper. It utilizes a Scott linkage mechanism to achieve a linear trajectory at the fingertip, employs a two-stage series-connected parallelogram linkage mechanism to maintain the orientation of the fingertip, and integrates multiple springs and stoppers to attain table-surface adaptive functionality, enabling both parallel grasping and asymmetric scooping. The gripper actively leverages collisions with the table surface to facilitate finger flexion, reducing the number of actuators required and achieving an adaptive underactuated effect.

ACKNOWLEDGEMENT

This research was supported by *the Foundation of Enhanced Student Research Training* (E-SRT), and the *Foundation of Open Research for Innovation Challenges* (ORIC), X-Institute.

REFERENCES

[1] Bicchi A. "Hands for Dexterous Manipulation and Robust Grasping: A Difficult Road Toward Simplicity," *IEEE Trans. on Robotics*, vol. 16, no. 6, pp. 652 – 662, 2000.

[2] Liu H., Meusel P., Hirzinger G. et al., "The Modular Multisensory DLR-HIT-Hand" *Mechanism and Machine Theory*, vol. 111, pp. 14 – 26, 2017.

[3] Birglen L., Gosselin C. M, "Kinetostatic Analysis of Underactuated Fingers," *IEEE Trans. on Robotics*, vol. 20, no. 2, pp. 211 – 221, 2004.

[4] Dollar A. M., Howe R. D., "The SDM Hand as a Prosthetic Terminal Device: A Feasibility Study," *IEEE Int. Conf. on Rehabilitation Robotics*, Noordwijk, Netherlands, pp. 978 – 983, Jun. 2007.

[5] Gosselin C. M., Laliberte T., "Underactuated Mechanical Finger with Return Actuation," *Patent, US5762390A*, Jun. 09, 1998.

[6] Feng K., Duan Z., Han C. et al., "Underactuated Finger Topology for Humanoid Robot Grasp," *Int. Conf. on Advanced Robotics and Mechatronics (ICARM)*, Tokyo, Japan, pp. 753 – 758, Jul. 2024.

[7] Chen S., Zhang B., Feng K. et al., "A Novel Geometrical Structure Robot Hand for Linear-parallel Pinching and Coupled Self-adaptive Hybrid Grasping," *IEEE/RSJ Int. Conf. on Intelligent Robots and Systems (IROS)*, Abu Dhabi, United Arab Emirates, pp. 3030 – 3035, Oct. 2024.

[8] Mosadegh B., Polygerinos P., Keplinger et al., "Pneumatic Networks for Soft Robotics that Actuate Rapidly," *Advanced Functional Materials*, vol. 24, no. 15, pp. 2163 – 2170, 2014.

[9] Deimel R., Brock O., "A Novel Type of Compliant and Underactuated Robotic Hand for Dexterous Grasping," *Int. J. of Robotics Research (IJRR)*, vol. 35, no. 1-3, pp. 161 – 185, 2016.

[10] Shepherd R. F., Ilievski F., Choi W. et al., "Multigait Soft Robot," *Proc. of the National Academy of Sciences (PNAS)*, vol. 108, no. 51, pp. 20400 – 20403, 2011.

[11] Majidi C., "Soft Robotics: A Perspective — Current Trends and Prospects for the Future," *Soft Robotics*, vol. 1, no. 1, pp. 5 – 11, 2014.

[12] Xie Z., Yuan F., Lu J. et al., "Octopus-inspired Sensorized Soft Arm for Environmental Interaction," *Science Robotics*, vol. 8, no. 84, Nov. 2023.

[13] Li W., Hu D., Yang L., "Actuation Mechanisms and Applications for Soft Robots: A Comprehensive Review," *Applied Sciences*, vol. 13, no. 16, 9255, 2023.

[14] Yoon D., Kim K., "Fully Passive Robotic Finger for Human-Inspired Adaptive Grasping in Environmental Constraints," *IEEE/ASME Trans. on Mechatronics*, vol. 27, no. 5, pp. 3841 – 3852, 2022.

[15] Tlegenov Y., Telegenov K., Shintemirov A., "An Open-source 3D Printed Underactuated Robotic Gripper," *IEEE/ASME Int. Conf. on Mechatronic and Embedded Systems and Applications (MESA)*, Senigallia, Italy, pp. 1 – 6, Sept. 2014.

[16] Luo C., Zhang W., Wang Z. et al., "Grasping Analysis and Experiment of a Linear-parallel and Self-adaptive Robot Hand," *J. of Mechanical Engineering*, vol. 57, no. 19, pp. 61 – 69, 2021.

[17] Deimel R., Brock O., "A Compliant Hand Based on A Novel Pneumatic Actuator," *IEEE Int. Conf. on Robotics and Automation (ICRA)*, Karlsruhe, Germany, pp. 2047 – 2053, May. 2013.

[18] Catalano M. G., Grioli G., Farnioli E. et al., "Adaptive Synergies for the Design and Control of the Pisa/IIT Soft Hand," *Int. J. of Robotics Research*, vol. 33, no. 5, pp. 768 – 782, 2014.

[19] Catalano M. G., Grioli G., Farnioli E. et al., "Exploitation of Environmental Constraints in Human and Robotic Grasping," *Int. J. of Robotics Research*, vol. 34, no. 7, pp. 1021 – 1038, 2015.